The Chaperonin TRIC Blocks a Huntingtin Sequence Element that promotes the Conformational Switch to Aggregation

Stephen Tam, Christoph Spiess, William Auyeung,
Lukasz Joachimiak, Bryan Chen, Michelle A. Poirier
and Judith Frydman

(Supplementary Figures)

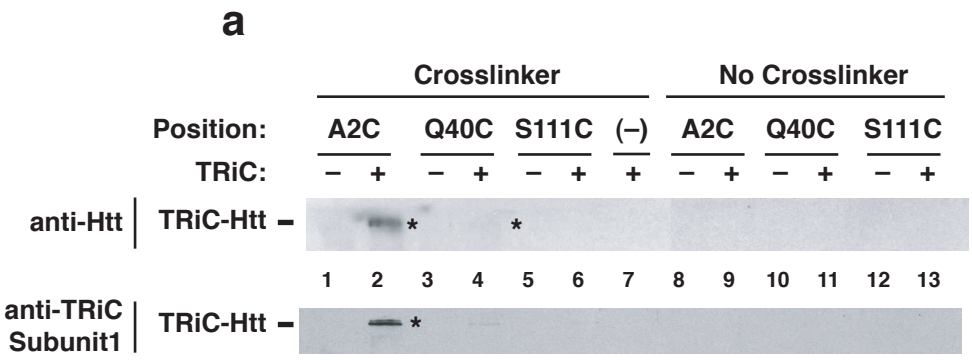
a
Crosslinker
No Crosslinker
Position:
A2C
Q40C
S111C
(–)
A2C
Q40C
S111C
TRiC:
– + – + – + + – + – + – +
anti-Htt
TRiC-Htt
*
*
1 2 3 4 5 6 7 8 9 10 11 12 13
anti-TRiC Subunit1
TRiC-Htt
*

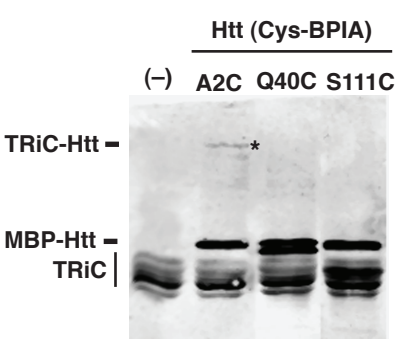
b
Htt (Cys-BPIA)
(–)
A2C
Q40C
S111C
TRiC-Htt
*
MBP-Htt
TRiC

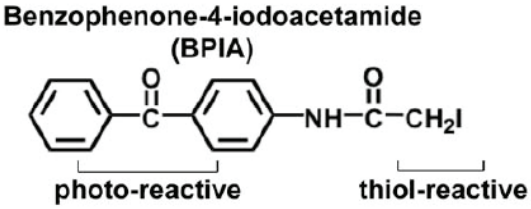
c
Benzophenone-4-iodoacetamide
(BPIA)
O
C
NH
O
C
CH2I
photo-reactive
thiol-reactive

Figure 1. Mapping the contact sites between Htt-exon1 and the chaperonin TRiC (a) High molecular TRiC-Htt crosslink band retained at top of the gel in blot shown in Fig. 1a of crosslink between TRiC and Htt-exon1. **(b)** Photo-crosslinked adducts detected by anti-Htt immunoblot analyses. The TRiC-Htt crosslink product is only observed when BPIA is positioned at the N-terminus (A2C; asterisk). **(c)** Structure of the crosslinker Benzophenone-4-iodoacetamide (BPIA).

a

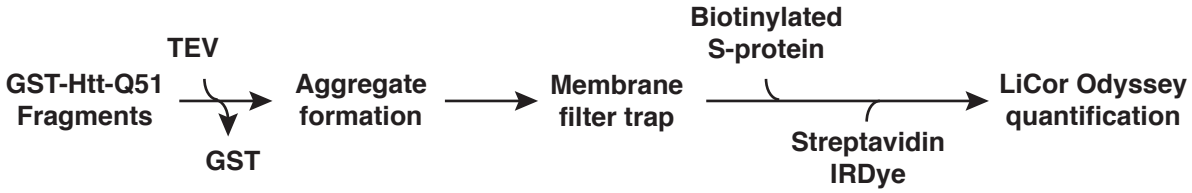
TEV
GST-Htt-Q51
Fragments
GST
Aggregate
formation
Membrane
filter trap
Biotinylated
S-protein
Streptavidin
IRDye
LiCor Odyssey
quantification

b

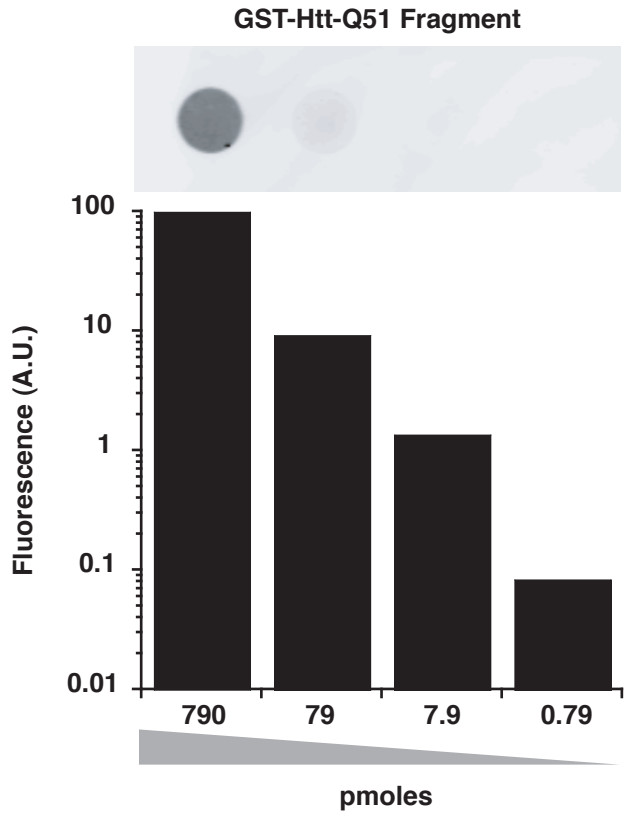
GST-Htt-Q51 Fragment
100
10
1
0.1
0.01
Fluorescence (A.U.)
790
79
7.9
0.79
pmoles

Figure 2. Quantification of Htt aggregates by infrared imaging. (a) Schematic representation of the detection of Htt aggregates. Aggregation of Htt is induced by protease cleavage of GST-Htt fusion protein. After trapping Htt aggregates on cellulose acetate filter, Htt is detected via the C-terminal S-tag by using biotinylated S-protein and Streptavidin IRDye; the signal is detected and quantified by infrared imaging on a LiCor Odyssey (see Online Methods). **(b)** Quantification of GST-fusion protein is linear over a wide concentration range. Serial dilutions of a GST-Htt-Q51 fragment were adsorbed by the filter trap assay to nitrocellulose membrane and the signal visualized (upper panel) and quantified (lower panel) using LiCor Odyssey infrared imaging technology. The signal is linear over at least four orders of magnitude.

a

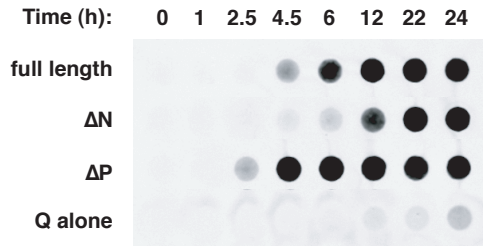
Time (h):
0
1
2.5
4.5
6
12
22
24
full length
ΔN
ΔP
Q alone

b

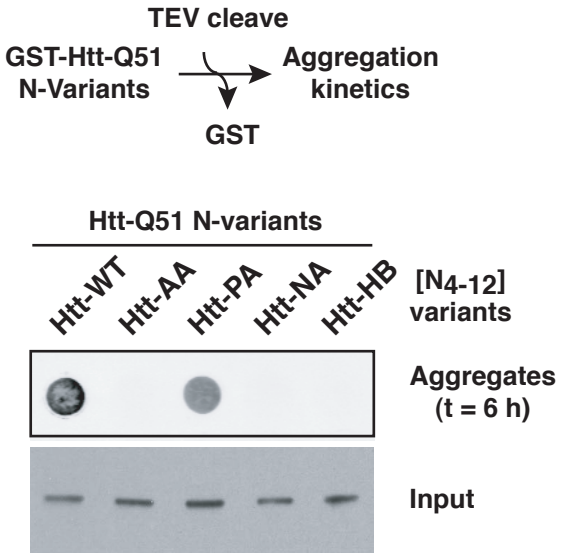
TEV cleave
GST-Htt-Q51
N-Variants
Aggregation
kinetics
GST
Htt-Q51 N-variants
Htt-WT
Htt-AA
Htt-PA
Htt-NA
Htt-HB
[N4-12]
variants
Aggregates
(t = 6 h)
Input

Figure 3. Raw Htt-exon1 aggregation quantification data. (a) *In vitro* GST-Htt-Exon1 aggregation assay of various Htt-exon1 domain truncations as described for Fig. 2b. Membrane trapped aggregates are visualized using LiCor Odyssey infrared imaging technology. The signal shown is the basis for the quantified data in Fig. 2b. All incubations were carried out and analyzed in the same experiment. **(b)** Aggregation of helical Htt variants fused to GST (Fig. 4a) was determined by filter-trap assay. Membrane trapped aggregates are visualized by LiCor Odyssey as described earlier (upper panel). The total protein input is visualized by SDS-PAGE and immunoblot analysis (lower panel). The signal is the basis for the quantified data in Fig. 4b. All incubations were carried out and analyzed in the same experiment.

a

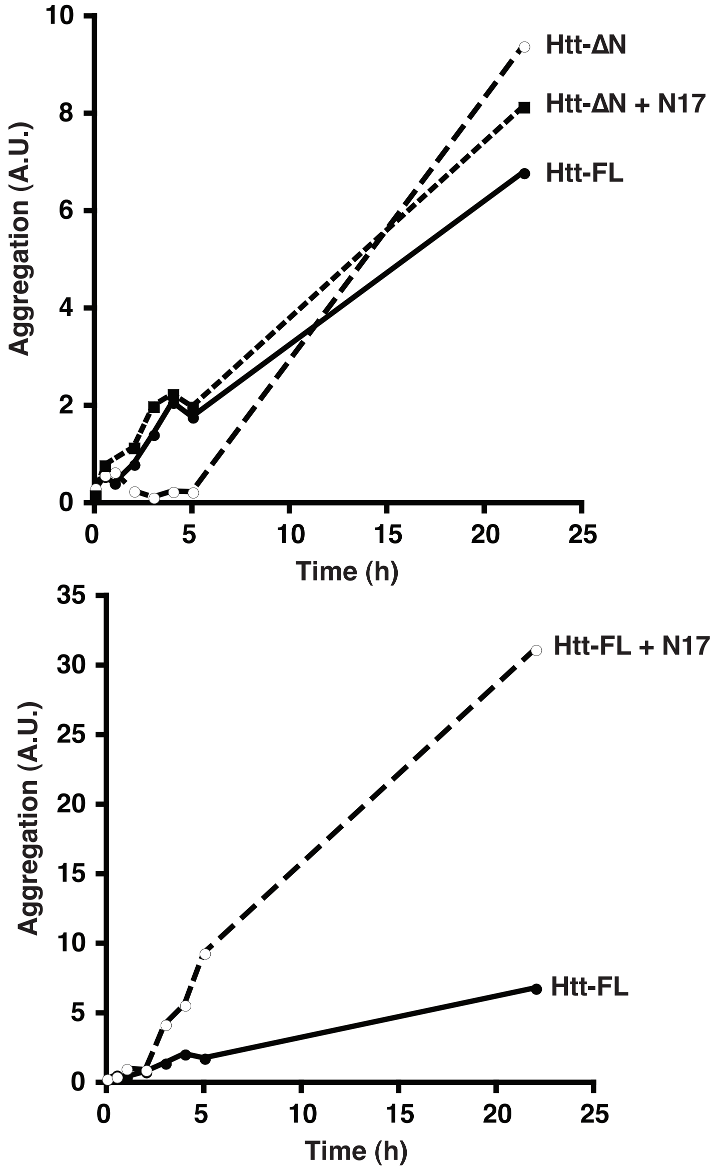

b

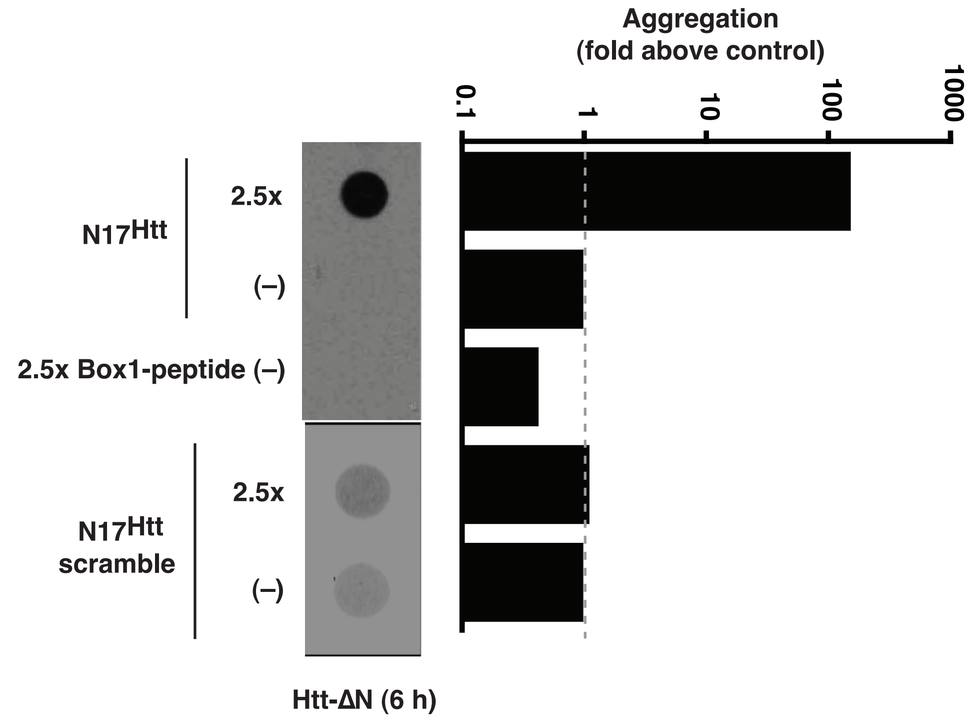

c

Full length-Htt Q51:
MATLEKLMKAFESLKSFQQQQQQQQQQQQQQQQQQQQQQQQQQQQQQQQQQQQQQQQQQQQQQQQQQQP
PPPPPPPPPPQLPQPPPQAQPLLPQPQPPPPPPPPPPPGPAVAEEPLHRPSVDTS**KETAAAKFERQHMDS**

DeltaN-Htt:
ESLKSFQQQQQQQQQQQQQQQQQQQQQQQQQQQQQQQQQQQQQQQQQQQQQQQQQQQPPPPPPPPPPPQ
LPQPPPQAQPLLPQPQPPPPPPPPPPPGPAVAEEPLHRPSVDTS**KETAAAKFERQHMDS**

DeltaP-Htt:
MATLEKLMKAFESLKSFQQQQQQQQQQQQQQQQQQQQQQQQQQQQQQQQQQQQQQQQQQQQQQQQQQPP
PSEPLHRPSVDTS**KETAAAKFERQHMDS**

DeltaNPC-Htt (polyQ):
ESLKSFQQQQQQQQQQQQQQQQQQQQQQQQQQQQQQQQQQQQQQQQQQQQQQQQQQPPPS**KETAAAKFE
RQHMDS**

Figure 4. The N-terminus of huntingtin specifically promotes rapid polyQ aggregation in a sequence-specific manner. **(a)** Trans addition of N17 peptide enhances Htt-exon1 aggregation kinetics. A synthetic peptide containing 17 amino acids of the N-terminal region ($N17^{Htt}$) was added to Htt-ΔN or to full-length Htt-exon1 and assayed at 0, 0. 5, 1, 2, 3, 4, 5, and 22 hrs. **(b)** Unlike N17, peptides corresponding to TRiC-VHL binding determinant Box1 or control peptides with a scrambled N17 sequence, fail to enhance Htt-ΔN aggregation kinetics. **(c)** Amino acid sequences immediately following the TEV protease recognition site of Htt-Exon1 fragments used to analyze the contribution of individual domains towards aggregation. In bold are the C-terminal S-tag moieties.

Figure S5
Tam et al.

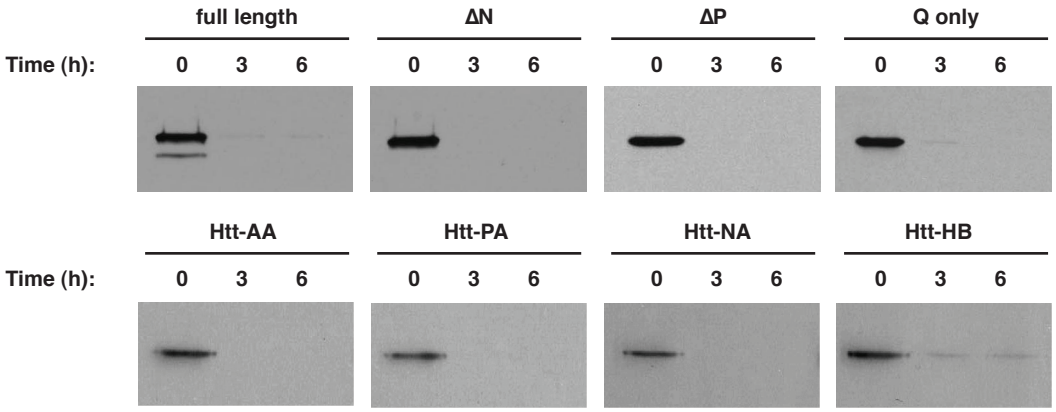

Figure 5. Efficient TEV cleavage kinetics of Htt-exon 1 bearing the indicated N-terminal helix variants or truncated fragments. Htt is detected via the C-terminal S-tag by using HRP-conjugated S-protein.

Figure S6
Tam et al.

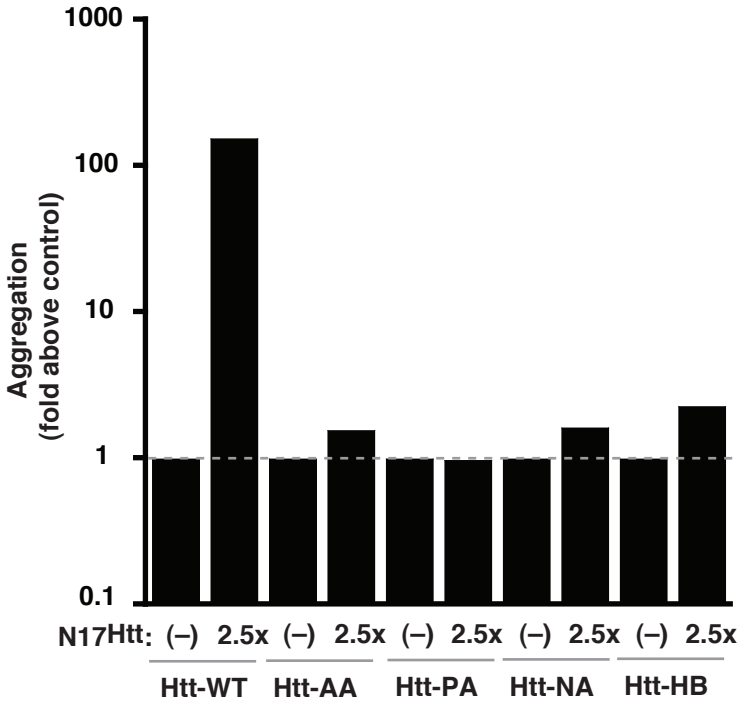

Figure 6. Trans addition of the N-terminus of huntingtin does not promote rapid aggregation of Htt-exon1 helical variants. Aggregation of Htt-exon 1 bearing the indicated N-terminal helix variants in response to trans addition of N17 peptide, carried out as described for Fig. 2c.

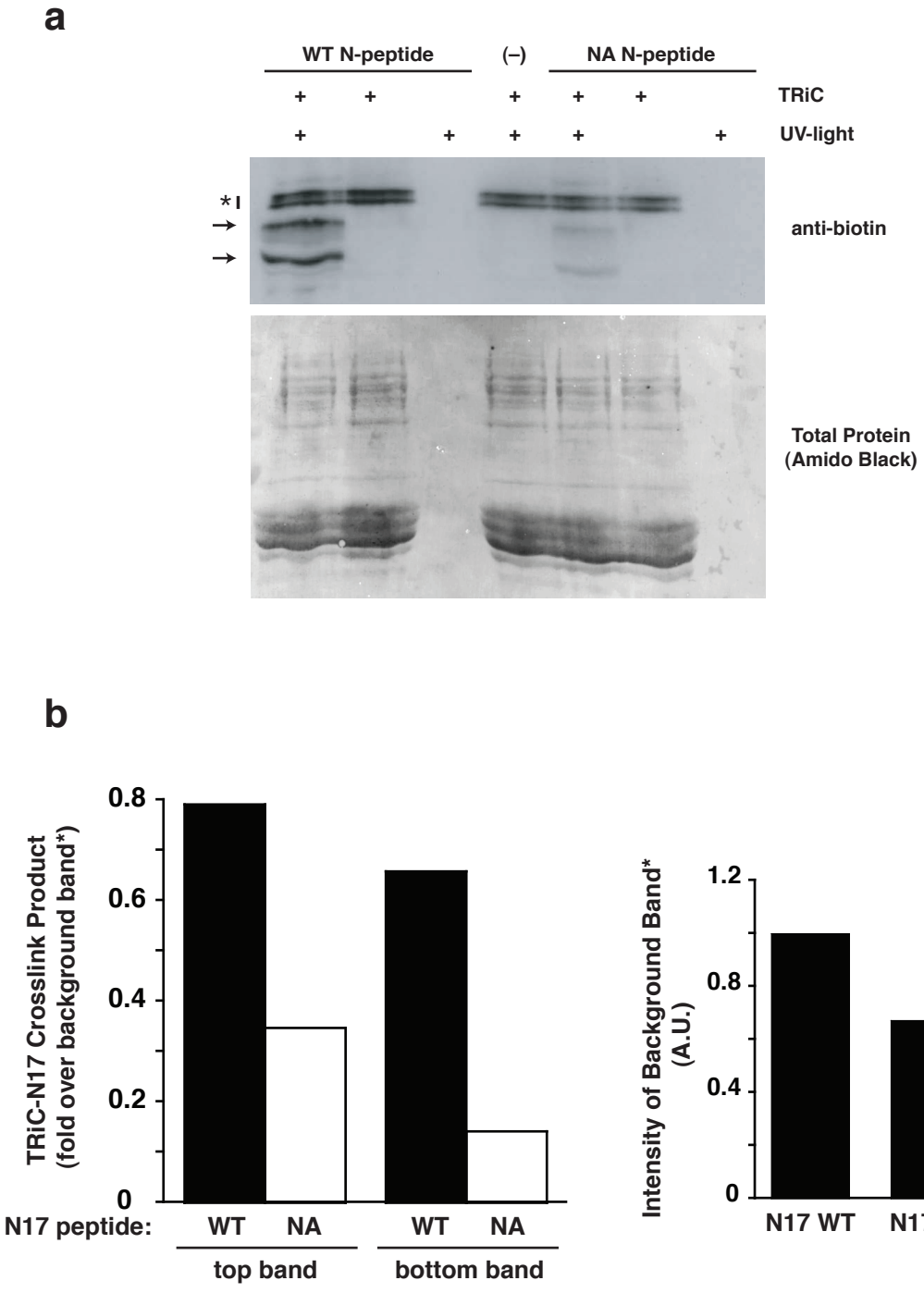
a
WT N-peptide
(–)
NA N-peptide
TRiC
UV-light
anti-biotin
Total Protein
(Amido Black)
b
TRiC-N17 Crosslink Product
(fold over background band*)
0.8
0.6
0.4
0.2
0
N17 peptide:
WT
NA
WT
NA
top band
bottom band
Intensity of Background Band*
(A.U.)
1.2
0.8
0.4
0
N17 WT
N17 NA

Figure 7. The hydrophobic surface of the N17 helix is the major Htt binding site for the chaperonin TRiC. **(a)** Top panel: Direct interaction of TRiC with N17 requires the hydrophobic face of the helix. Crosslinking to TRiC was tested for the wild type N17 peptide (N17-WT) or with a peptide carrying alanine substitutions in the hydrophobic side of the N17-helix (N17-NA). TRiC- and UV-dependent adducts were detected probing for the biotin moiety of the peptide. Non-specific background signals are labeled with an asterisk. (-): no peptide control. Results representative of at least three independent experiments are shown. Bottom panel: Amido black-stained membrane from above shows equivalent sample loading. **(b)** Left panel: quantification of crosslink product using background signal as loading control. Right panel: quantification of background signal.


TEV site
S-tag
GST
Htt-Exon1-POLYQ
N17
GST-Htt
(N17 WT or NA)
GSH-
beads
cell
extract
wash/elute
• SDS-PAGE
• Immunoblot
Input Htt
GST
GST-WT Htt
GST-NA Htt
Anti-S-tag
Bound TRiC
Input TRiC
GST
GST-WT Htt
GST-NA Htt
Anti-TRiC

Figure 8. The hydrophobic surface of the N17 helix is a key TRiC-binding element within the context of the entire Htt-exon1 protein. Pulldown assays were carried out using Htt-exon1 carrying a C-terminal S-tag and an N-terminal GST-moiety as described in Tam et al. Isolation of endogenous yeast TRiC that interacted with Htt was carried out by GST pulldown of equimolar amounts of purified wild type GST-huntingtin exon1 (GST-WT) and GST-huntingtin exon1 containing NA mutations within the N-terminus (GST-NA). GST fusions were prebound to glutathione-sepharose beads and incubated with yeast lysate containing endogenous TRiC. Associated TRiC was detected by immunoblotting. Inputs were detected with an antibody against the C-terminal S-tag on both GST-WT and GST-NA.

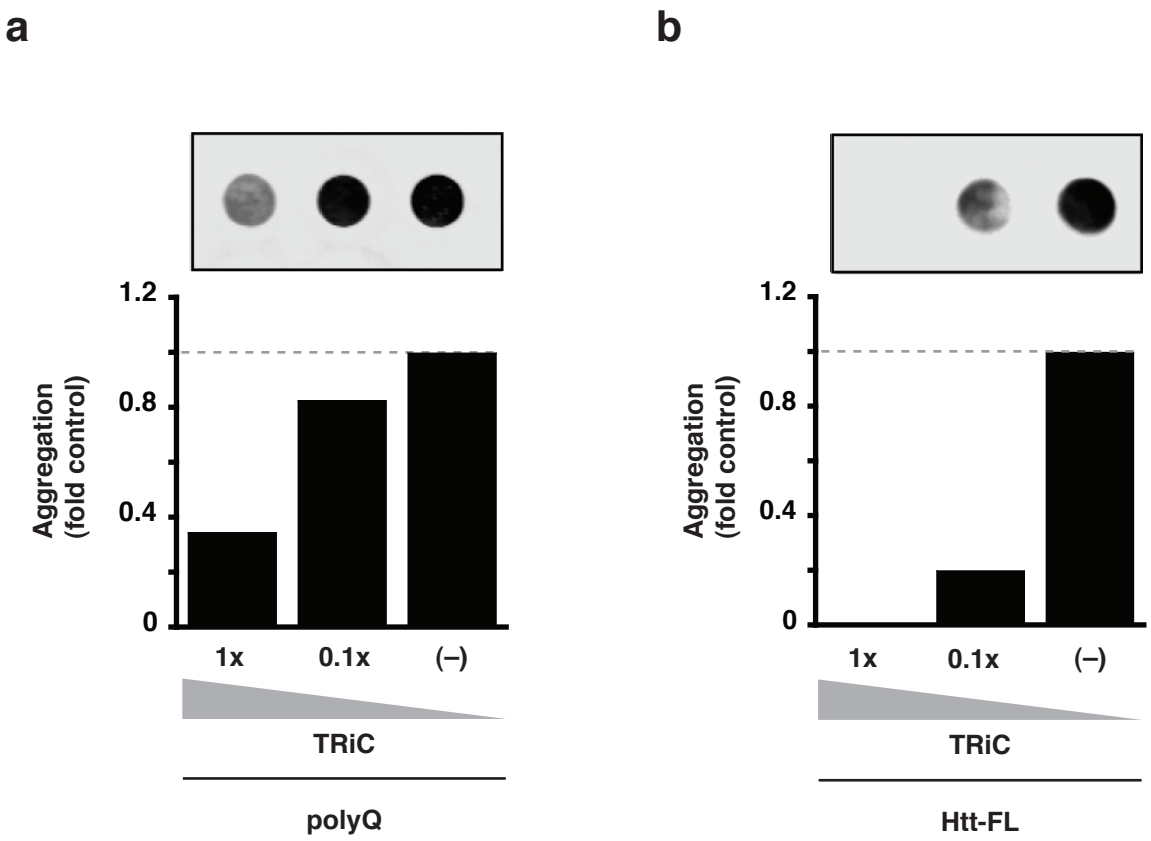
a
b
Aggregation (fold control)
1.2
0.8
0.4
0
1x
0.1x
(–)
TRiC
polyQ
Htt-FL

Figure 9. The chaperonin TRiC does not efficiently suppress polyQ aggregation to the same extent as full length Htt-exon 1. Purified TRiC fails to efficiently neutralize the aggregation of polyQ compared to its efficient neutralization of aggregation of Htt-exon 1. Representative results of at least three independent experiments are shown.